HHS Public Access

Author manuscript

Oncogene. Author manuscript; available in PMC 2018 August 12.

Published in final edited form as:

Oncogene. 2018 May ; 37(18): 2379–2393. doi:10.1038/s41388-017-0101-3.

p53 isoforms regulate premature aging in human cells

Natalia von Muhlinen[1], **Izumi Horikawa**[1], **Fatima Alam**[1], **Kazunobu Isogaya**[1], **Delphine Lissa**[1], **Borek Vojtesek**[2], **David P Lane**[3], and **Curtis C. Harris**[1]

[1]Laboratory of Human Carcinogenesis, National Cancer Institute, NIH, Bethesda, MD, 20892

[2]Regional Centre for Applied and Molecular Oncology, Masaryk Memorial Cancer Institute, Brno 65653, Czech Republic

[3]Department of Microbiology, Tumor and Cell Biology (MTC), Karolinska Institutet, Box 280, SE-171 77 Stockholm, Sweden

Abstract

Cellular senescence is a hallmark of normal aging and aging-related syndromes, including the premature aging disorder Hutchinson-Gilford Progeria Syndrome (HGPS), a rare genetic disorder caused by a single mutation in the *LMNA* gene that results in the constitutive expression of a truncated splicing mutant of lamin A known as progerin. Progerin accumulation leads to increased cellular stresses including unrepaired DNA damage, activation of the p53 signaling pathway and accelerated senescence. We previously established that the p53 isoforms Δ133p53 and p53β regulate senescence in normal human cells. However, their role in premature aging is unknown. Here, we report that p53 isoforms are expressed in primary fibroblasts derived from HGPS patients, are associated with their accelerated senescence and that their manipulation can restore the replication capacity of HGPS fibroblasts. We found that in near-senescent HGPS fibroblasts, which exhibit low levels of Δ133p53 and high levels of p53β, restoration of Δ133p53 expression was sufficient to extend replicative lifespan and delay senescence, despite progerin levels and abnormal nuclear morphology remaining unchanged. Conversely, Δ133p53 depletion or p53β overexpression accelerated the onset of senescence in otherwise proliferative HGPS fibroblasts. Our data indicate that Δ133p53 exerts its role by modulating full-length p53 (FLp53) signaling to extend the replicative lifespan and promotes the repair of spontaneous progerin-induced DNA double strand breaks (DSBs). We showed that Δ133p53 dominant-negative inhibition of FLp53 occurs directly at the p21/CDKN1A and miR-34a promoters, two p53-senescence associated genes. In addition, Δ133p53 expression increased expression of the DNA repair RAD51, likely through upregulation of E2F1, a transcription factor that activates RAD51, to promote repair of DSBs. In summary, our data indicate that Δ133p53 modulates p53 signaling to repress progerin-

CORRESPONDENCE TO: Curtis C. Harris, MD; harrisc@mail.nih.gov, Laboratory of Human Carcinogenesis, Center for Cancer Research, National Cancer Institute, National Institutes of Health, Bldg. 37, Rm. 3068, 37 Convent Drive, Bethesda, Maryland 20892-4258. Phone: 301-496-2048. Fax: 301-496-0497.

AUTHOR CONTRIBUTIONS: N.V.M., F.A., K.I. AND D.L. performed the experiments. I.H. provided essential expertise and reagents. N.V.M., I.H., B.V., D.P.L. and C.C.H. coordinated the study and wrote the manuscript. C.C.H. was responsible for the overall study.

CONFLICT OF INTEREST: The authors have no conflict of interest.

induced early onset of senescence in HGPS cells. Therefore, restoration of Δ133p53 expression may be a novel therapeutic strategy to treat aging-associated phenotypes of HGPS *in vivo*.

Keywords

Δ133p53; premature aging; HGPS; cellular senescence; DNA damage; DNA repair; RAD51; p53; p53 isoforms; E2F1; aging

INTRODUCTION

Cellular senescence, a state of growth arrest, can be induced by telomere shortening (known as replicative senescence)[1] or other cellular stresses such as non-telomeric DNA damage[2] in normal human cells. Senescence is closely associated with normal development[3] and organismal aging, as evidenced by the accumulation of senescent cells *in vivo*, which may compromise tissue functionality and limit the regeneration potential of adult stem cells[4, 5]. Furthermore, senescence is one of the hallmarks of premature aging disorders such as Hutchinson-Gilford Progeria Syndrome (HGPS)[6, 7], a rare genetic disorder that causes premature aging[8]. HGPS children, who appear normal at birth, show symptoms of accelerated aging including growth retardation, skin atrophy and cardiovascular complications within the first year of age[9]. The major cause of death of HGPS children, who survive to an average age of 13.5 years old, is vascular disease[10].

HGPS is caused by an autosomal *de novo* mutation in the *LMNA* gene that generates an alternative cryptic splice site that leads to the production of the disease-causing truncated prelamin A known as progerin[11, 12]. Accumulation of progerin induces several cellular defects including alterations of the nuclear lamina, abnormal nuclear morphology, impairment of Nrf2 pathway leading to an increase of reactive oxygen species (ROS), alterations in transcriptional activity and defective DNA replication and DNA repair[13–20]. Spontaneous unrepaired DNA double strand breaks (DSBs), one of the main cellular features of HGPS fibroblasts, accumulate due to sequestration of DNA replication and DNA repair factors by progerin, causing defective DNA repair and genomic instability in HGPS cells *in vitro* and *in vivo*[21–24]. As a result, genomic instability induces a series of DNA damage checkpoints that lead to p53 signaling activation, early replication arrest and premature aging symptoms[25, 26].

The p53 signaling pathway is a central regulator of replicative senescence. The human *TP53* gene expresses at least 13 isoforms including full-length p53 (FLp53) as a result of alternative splicing, alternative promoter usage or alternative transcription start site[27]. We previously reported that the naturally-occurring p53 isoforms Δ133p53 and p53β are physiological regulators of cellular proliferation and senescence in normal human fibroblasts *in vitro*[28], in human T lymphocytes *in vitro* and *in vivo*[29], in human brain astrocytes *in vitro* and *in vivo*[30] and in induced pluripotent stem cells (iPSC)[31]. Δ133p53, an N-terminally truncated isoform initiated by usage of methionine in codon 133 in mRNA transcribed from the *TP53* promoter 2[32], is present only in humans and higher primates[30]. Δ133p53 inhibits senescence by inhibiting the expression of the downstream p53-target genes *p21/CDKN1A* and miR-34a[28], consistent with its dominant-negative inhibition of full-length p53 (FLp53).

In contrast, p53β, a C-terminally truncated isoform that cooperates with FLp53, enhances senescence in several normal cell types[28–30]. While FLp53 is regulated by proteasomal degradation[33, 34], Δ133p53 protein levels are modulated by chaperone-assisted selective autophagy during replicative senescence of normal cells[35], and p53β is negatively regulated at the *mRNA* level by the splicing factor SRSF3[36]. Whether p53 isoforms have a role in the early onset of senescence associated with progerin accumulation in HGPS fibroblasts remains currently unknown.

Previous studies showed that Δ113p53, an N-terminally truncated p53 isoform expressed in zebrafish, promotes DNA DSB repair in zebrafish embryos by modulating the expression of DNA DSB repair factors[37], such as RAD51, the expression of which is sufficient for effective homologous recombination (HR) and to maintain genomic stability[38]. Furthermore, RAD51 expression is regulated by E2F1, a transcription factor repressed by FLp53[39, 40]. However, the role of human Δ133p53 during the early induction of senescence associated with defective DNA repair in premature aging is unknown.

Here, we show that Δ133p53 and p53β isoforms are key regulators of the accelerated senescence characteristic of HGPS fibroblasts. Depletion of Δ133p53 or overexpression of p53β induce the early onset of senescence in otherwise proliferative HGPS cells, which is in contrast to extension of replicative lifespan and inhibition of senescence by restoration of Δ133p53 expression in near-senescent HGPS fibroblasts. Our mechanistic studies show that Δ133p53 overexpression dominant-negatively inhibits p53 signaling pathway and represses the expression of senescence-associated secretory phenotype (SASP) pro-inflammatory cytokines. Furthermore, Δ133p53 leads to decreased DNA damage foci in HGPS fibroblasts. Thus, our study identifies p53 isoforms as novel regulators of premature aging, and proposes Δ133p53 as a potential therapeutic target to address one of the most critical features of HGPS patients, namely, the premature aging of HGPS children.

RESULTS

p53 isoforms regulate replicative senescence in HGPS fibroblasts

We first investigated the expression of p53 isoforms during serial passaging *in vitro* of cultured primary human fibroblasts generated from two HGPS patients (AG11513 and HGADFN188, Supplementary Table S1). These cell strains, which are derived from young HGPS patients, replicate for approximately 10 passages in culture before approaching cellular replicative arrest. To measure expression of p53 isoform proteins, western blot using the polyclonal antibodies MAP4 or TLQi9 to specifically detect the Δ133p53 or p53β isoforms[28, 32], respectively, was performed in HGPS fibroblasts at early passage or approaching senescence. Consistent with its negative regulation of senescence in normal human cells[28–30], Δ133p53 was expressed in proliferative HGPS cells but its protein levels were decreased (Figure 1A) in HGPS fibroblasts that expressed progerin (Figure S1) and had reached cellular proliferation arrest, as evidenced by increased cellular staining with senescence-associated-β-galactosidase (SA-β-gal) (Figure S2). In contrast, expression of p53β, a co-activator of FLp53 that enhances senescence in several normal cell types[28–30], was upregulated at the *mRNA* (Figure S3A) and protein levels upon senescence of HGPS fibroblasts (Figure S3B). These data show that the p53 expression profile at cellular

senescence is conserved not only among normal cell types that reach cellular growth arrest due to telomere shortening associated with serial passaging[28–30], but also in diseased HGPS cells that become senescent prematurely due to progerin-induced cellular stresses.

Next, we recapitulated the expression profile of p53 isoforms found in senescent cells (diminished Δ133p53 and enhanced p53β) in two different cell strains of proliferative HGPS fibroblasts (AG11513 and HGADFN188) to investigate whether it would modulate senescence. Expression of Δ133p53 was abrogated using two different isoform-specific siRNAs[28]. Δ133p53 knockdown was confirmed by western blot, whereas changes in FLp53 were not detected (Figure 1B). Cells transfected with Δ133p53 siRNAs exhibited an early onset of senescence as evidenced by increased SA-β-gal staining compared to control-transfected cells (Figure 1C and 1D). Increased *mRNA* expression of the senescence-associated p53-target *p21/CDKN1A* as well as *IL-6* and *IL-8*, two SASP pro-inflammatory cytokines, were also observed in cells depleted of Δ133p53 (Figure 1D). These data indicate that loss of Δ133p53 in HGPS fibroblasts induces cellular senescence associated with increased transcription of p53 target genes and induction of SASPs.

Enforced expression of lentiviral-driven FLAG-tagged p53β in proliferative HGPS fibroblasts (AG11513 and HGADFN188) was confirmed by western blot using anti-FLAG antibody (Figure S3C). Similar to knockdown of Δ133p53 (Figure 1B-D), overexpression of p53β resulted in a rapid onset of senescence as evidenced by decreased SA-β-gal staining compared to control-transduced cells, which continued to proliferate (Figures S3D and S3E).

Altogether, these results reveal that Δ133p53 and p53β isoforms are negative and positive modulators of replicative senescence in HGPS fibroblasts, respectively.

Δ133p53 and p53β are regulated by chaperone-assisted selective autophagy and alternative splicing, respectively, in HGPS fibroblasts

While FLp53 is regulated by proteasomal degradation[33, 34], Δ133p53 is regulated at the protein level by chaperone-assisted selective autophagy, a specific regulatory process in which the E3 ligase STUB1/CHIP1 stabilizes Δ133p53 to prevent its degradation[35]. To test whether this mechanism is conserved in HGPS fibroblasts, we first treated HGPS cells with the pharmacological inhibitor of autophagy bafilomycin A1 (BafA1)[41] or with DMSO as control. Autophagy inhibition in BafA1-treated cells, confirmed by accumulation of the autophagy-related proteins p62 and LC3B, resulted in increased Δ133p53 isoform in HGPS fibroblasts compared to control-treated cells (Figure 2A).

We next examined STUB1 protein levels in serially-passaged HGPS fibroblasts. STUB1 protein was diminished in senescent HGPS fibroblasts compared to proliferative cells (Figure 2B), consistent with results in normal human fibroblasts[35]. To test whether STUB1 regulates Δ133p53 levels as in normal human fibroblasts, we treated proliferative HGPS (AG11513 and HGADFN188) fibroblasts with two siRNAs against STUB1[35]. The siRNA-mediated depletion of STUB1, confirmed by western blot, resulted in diminished Δ133p53 protein levels (Figure 2C), indicating that STUB1 stabilizes Δ133p53. Importantly, knockdown of STUB1 also promoted the early onset of senescence in otherwise proliferative HGPS fibroblasts, as shown by increased SA-β-gal staining (Figure 2D and 2E). Overall,

because siRNA-mediated downregulation of STUB1 reproduced the features of senescent HGPS fibroblasts, that STUB1 regulation of Δ133p53 and senescence is conserved in HGPS fibroblasts. In conclusion, these data, together with our previous results[35], indicate that STUB1 is critical to maintain Δ133p53 expression and to prevent its degradation by selective autophagy in HGPS fibroblasts.

In contrast to chaperone-assisted selective autophagy of Δ133p53 protein, p53β is negatively regulated at the *mRNA* level by the splicing factor SRSF3 in normal cells[36]. We examined endogenous expression of SRSF3 in proliferative and senescent HGPS (AG11513 and HGADFN188) fibroblasts. SRSF3 protein levels were diminished in senescent HGPS cells (Figure S4A), which was inversely correlated with the high levels of p53β *mRNA* detected in senescent HGPS fibroblasts (Figure S3A). siRNA-mediated depletion of SRSF3, confirmed by western blot (Figure S4B), resulted in increased p53β expression at the protein (Figure S4B) and mRNA (Figure S4C) levels, consistent with negative regulation of p53β by SRSF3. Diminished SRSF3 also led to increased SA-β-gal staining and enhanced *p21/CDKN1A* mRNA expression (Figure S4D-F), consistent with an early onset of senescence in otherwise proliferative HGPS fibroblasts. In conclusion, our data show that the mechanism that regulates p53β expression via alternative splicing during senescence is conserved among normal primary fibroblasts and primary fibroblasts from HGPS patients.

Restoration of Δ133p53 expression delays HGPS fibroblasts from becoming senescent

To investigate whether restoration of Δ133p53 expression rescues the senescence of HGPS fibroblasts, near-senescent HGPS fibroblasts derived from two patients (AG11513 and AG01972) were transduced with lentiviral supernatants to overexpress Δ133p53 or a vector control. Ectopic expression of the Δ133p53 lentiviral vector was confirmed by immunoblot (Figure 3A). Overexpression of Δ133p53 was approximately two-fold higher than levels of endogenous Δ133p53 in proliferative AG11513 (HGPS) cells (Supplementary Figure S5). While vector control-transduced AG11513 HGPS cells reached cellular growth arrest after approximately 10 PDLs, Δ133p53-overexpressing HGPS cells continued to proliferate for approximately 30 PDLs (Figure 3B). AG01972 HGPS fibroblasts transduced with a control vector approached senescence within 5 PDLs, while cells overexpressing Δ133p53 continued to replicate for approximately 15 PDLs. These differences in the extension of replicative lifespan might be a result of the older age of the patient from which AG01972 cells are derived from (Supplementary Table S1). Consistent with inhibition of senescence, reconstitution of Δ133p53 expression in both AG11513 and AG01972 fibroblasts led to decreased SA-β-gal staining (Figure 3C and S6) as well as diminished *mRNA* expression of the SASP pro-inflammatory cytokines *IL-6* and *IL-8* (Figure 3D) compared to proliferative control vector-transduced cells. After Δ133p53-expressing AG11513 (HGPS) cells approached proliferation arrest, they expressed similar levels of SASPS compared to senescent control-transduced cells (Supplementary Figure S7).

Because accelerated senescence is associated with the effects of progerin accumulation in HGPS, we examined expression of progerin and the nuclear morphology of Δ133p53-expressing HGPS fibroblasts. Neither *mRNA* (Figure 3E) nor protein levels (Figure 3A) of progerin were significantly changed by Δ133p53 expression. Analysis of the nuclear

architecture by immunofluorescence showed no significant changes in nuclear shape in Δ133p53-expressing cells (Figure 3F and 3G) compared to control-transduced cells. Altogether, these results indicate that Δ133p53 expression extends the replicative lifespan and delays the onset of senescence in HGPS fibroblasts via a mechanism that is downstream of progerin alternative splicing or progerin-induced abnormal nuclear morphology.

Δ133p53 dominant-negatively inhibits p53 signaling in HGPS fibroblasts

Because Δ133p53 abrogates the activation of p53-target genes in several normal cell types[28, 32], possibly through binding to FLp53[42, 43], we hypothesized that Δ133p53 may delay the onset of senescence by inhibiting FLp53 in HGPS fibroblasts. First, we analyzed the expression of FLp53 and its characteristic activating phosphorylation at serine 15 (pS15-p53)[44] in Δ133p53-expressing HGPS cells (AG11513 and AG01972). Both FLp53 and pS15-p53 were accumulated in fibroblasts expressing Δ133p53 compared to control-transduced cells (Figure 4A). Thus, we hypothesized that accumulation of FLp53 may be due to physical interaction between Δ133p53 and FLp53. Overexpressed FLAG-tagged Δ133p53 co-immunoprecipitated FLp53 in HGPS fibroblasts (Figure 4B). Consistent with inhibition of the p53 signaling pathway, Δ133p53 expression resulted in decreased *p21/CDKN1A* mRNA (Figure 4C) and miR-34a expression (Figure 4D), two p53-target genes associated with cellular senescence[28, 45, 46] compared to control-transduced cells. These data indicate that Δ133p53 delays the onset of senescence in HGPS at least partially by interacting with FLp53 to dominant-negatively repress p53 signaling, which is aberrantly activated in HGPS due to progerin accumulation.

Δ133p53 promotes DNA repair of DNA double strand breaks in HGPS fibroblasts likely due to increased expression and recruitment of the DNA repair factor RAD51 to sites of DNA damage

Cellular accumulation of DNA damage is a hallmark of HGPS fibroblasts[23–25], which harbor increased spontaneous double-strand breaks (DSBs) compared to normal fibroblasts[47] due to accumulation of progerin[25]. The N-terminally truncated zebrafish p53 isoform Δ113p53 promotes DNA DSB repair in zebrafish embryos[37]. To investigate qualitative and quantitative changes in the DNA damage response upon expression of Δ133p53 in HGPS fibroblasts, we performed immunofluorescence staining of phosphorylated histone H2AX (γH2AX), which occurs specifically at sites of DSBs[48]. Immunostained HGPS fibroblasts expressing Δ133p53 or a control vector were examined by confocal microscopy and the number of γH2AX-positive foci was quantified. While normal human fibroblasts were reported to have at most only a few spontaneous γH2AX foci[2], HGPS cells had 10.5 ± 3.5 (mean ± SD) γH2AX foci per cell, consistent with previous reports[25]. HGPS fibroblasts overexpressing Δ133p53 showed a significant decrease in the number of DSB foci to 6.5 ± 2.2 (mean ± SD) (Figure 5A and Supplementary Figure S8). Therefore, these data indicate that Δ133p53 expression ameliorates DNA damage in HGPS fibroblasts.

Accumulation of spontaneous DNA damage foci may arise from defective DNA repair by homologous recombination (HR)[49] likely due to impaired recruitment of RAD51, a DNA repair factor essential for effective HR[38, 50], to sites of DNA damage foci[51]. FLp53 and

Δ133p53 modulate HR by repressing and inducing the expression of RAD51, respectively[37, 40, 52]. We examined whether Δ133p53 modulates expression of RAD51 in HGPS cells (AG11513 and HGADFN188) transduced with a control- or Δ133p53-lentiviral vector. Quantitative RT-PCR and western blot experiments showed that both mRNA (Figure 5B) and protein (Figure 5C) levels of RAD51 were increased in Δ133p53-expressing compared to control-transduced HGPS cells.

In HGPS, defective DNA repair of DSBs is caused in part by impaired recruitment of RAD51 to sites of DNA damage[51]. Therefore, we investigated if Δ133p53 expression influenced the localization of RAD51 at sites of DNA damage. We used confocal microscopy to quantify γH2AX and RAD51 co-localization in co-immunostained HGPS fibroblasts expressing Δ133p53 or a control vector. Our data showed that while most γH2AX-positive foci did not co-localize with RAD51 in control-transduced cells, approximately 50% of the fewer γH2AX foci were stained positive for RAD51 in Δ133p53-expressing cells (Figure 5D and 5E). In conclusion, these results support a role for Δ133p53 in promoting DNA DSB repair in HGPS cells by upregulating RAD51 expression. Our data indicate that higher expression of RAD51 in Δ133p53-expressing HGPS fibroblasts may result in higher recruitment of RAD51 to γH2AX-positive DSBs and thus, more effective DNA repair of DSB foci.

Overexpression of Δ133p53 increases RAD51 expression through its repression of FLp53 and upregulation of E2F1

Next, we investigated the mechanistic basis for enhanced expression of RAD51 in Δ133p53-transduced cells. Previous studies showed that FLp53 binds to RAD51 and the binding site was mapped between amino acids 94 and 160 of FLp53[53]. Overexpression of FLAG-Δ133p53, which harbors amino acids 133-160 of FLp53, did not co-immunoprecipitate RAD51 in BJ fibroblasts (Supplementary Figure S9). Thus, our data showed that Δ133p53 does not bind to RAD51.

Accumulation of RAD51 at the mRNA level suggests Δ133p53 may increase transcriptional activation of RAD51 dependently or independently of FLp53. To test these hypotheses, we transduced p53-null fibroblasts (041−/−) and lung cancer cells (H358), which lack FLp53 and its isoforms, with Δ133p53 lentivirus. Our data showed no significant change in RAD51 levels upon overexpression of Δ133p53 isoform in p53-null fibroblasts (Figure 6A) or p53-null lung cancer cells (Supplementary Figure S10). We next tested the effects of siRNA-mediated knockdown of FLp53 in AG11513 (HGPS) fibroblasts expressing control- or Δ133p53-lentiviral vectors. We confirmed depletion of FLp53 in siRNA-transfected fibroblasts, while levels of Δ133p53 remained unchanged (Figure 6B). Consistent with our results shown in Figure 4C, overexpression of Δ133p53 dominant-negatively inhibited mRNA levels of the p53-target gene p21/CDKN1, and knockdown of FLp53 in these cells significantly decreased the expression of p21/CDKN1A (Figure 6C). In contrast, siRNA-mediated depletion of FLp53 in control-transduced HGPS fibroblasts was sufficient to significantly increase RAD51 expression at the mRNA and protein levels, and overexpression of Δ133p53 did not have any additional effect (Figure 6B and 6D). These

results indicate that the increase of RAD51 upon overexpression of Δ133p53 in HGPS cells occurs in a FLp53-dependent manner.

Previous studies showed that FLp53 may repress RAD51 expression either by binding to its promoter[37, 40] or through repression of E2F1[54], an activator of RAD51 transcription[39]. Our analysis of publicly available chromatin immunoprecipitation (ChIP)-sequencing data sets showed that FLp53 does not bind to RAD51 promoter, in contrast to two positive control loci, including p21/CDKN1A and miR34-a (Supplementary Figure S11 and Table S2). Furthermore, our ChIP-qPCR analysis of FLp53 binding element showed significant binding to p21/CDKN1A loci but not to RAD51 loci (Supplementary Figure S12).

Because E2F1 is repressed by FLp53[54], we hypothesized that it might be upregulated by expression of Δ133p53 due to its dominant-negative inhibition of FLp53. First, we confirmed that depletion of FLp53 by siRNA resulted in increased E2F1 mRNA levels (Figure 6E). Consistent with our hypothesis, our data showed that E2F1 mRNA levels are significantly increased in Δ133p53-expressing AG11513 (HGPS) fibroblasts compared to control-transduced cells (Figure 6E).

Our database search analysis showed that consistent with previous publications[55], E2F1 binds to RAD51 promoter (Supplementary Figure S11 and Table S2). Thus, we hypothesized that enhanced RAD51 expression in Δ133p53-expressing HGPS fibroblasts may be due to upregulation of E2F1 by Δ133p53. Our results showed that siRNA-mediated depletion of E2F1, confirmed by quantitative RT-PCR (Figure 6E), reverted the increase in RAD51 mRNA expression in Δ133p53-expressing fibroblasts. Altogether, we concluded that overexpression of Δ133p53 increases RAD51 expression through its repression of FLp53 and upregulation of E2F1, ultimately leading to increased DNA repair likely due to enhanced RAD51 recruitment to sites of DNA double strand breaks.

DISCUSSION

In this study, we showed that p53 isoforms are endogenous regulators of the accelerated aging phenotype associated with the cytotoxic effects of progerin expression in primary fibroblasts derived from HGPS patients. As we previously reported in serially-passaged normal human cells undergoing replicative senescence in culture[28–30], Δ133p53 and p53β, whose expression are regulated by mechanisms that are conserved in HGPS fibroblasts[35, 36], inhibit and induce cellular senescence, respectively.

In HGPS, accumulation of progerin causes several aging-associated cellular phenotypes, including increased DNA damage, chronic oxidative stress and the early onset of senescence[13, 23–25]. Our report shows that although restoration of Δ133p53, otherwise diminished in near-senescent HGPS fibroblasts, did not affect progerin expression or its associated abnormal nuclear morphology, it was nevertheless sufficient to extend their lifespan and rescue their senescent phenotype. Thus, Δ133p53 inhibits accelerated senescence by a mechanism that is downstream of progerin expression and nuclear abnormalities in HGPS. Here, we presented evidence that despite stabilization and S15-phosphorylation of FLp53, Δ133p53 overexpression dominant-negatively inhibits p53-

mediated senescence and its downstream targets *p21/CDKN1A* and miR-34a in HGPS fibroblasts. Furthermore, our study showed that Δ133p53 activates RAD51, a DNA repair factor which expression level of which is a determinant of homologous recombination activity[38], to promote repair of spontaneous DSBs in HGPS fibroblasts. The mechanisms by which Δ133p53 increases RAD51 expression may be cell type and/or context-dependent. Δ113p53, an N-terminally truncated p53 isoform in zebrafish, have been previously reported to modulate HR by transcriptionally regulating RAD51 in response to DNA damage induced by γ-irradiation[37]. Zebrafish Δ113p53 and human Δ133p53, endogenously expressed in an immortalized cancer cell line, promote HR by a gain-of-function to directly transactivate RAD51 in a p53-independent manner[37]. Our data indicate that expression of Δ133p53 in HGPS leads to enhanced RAD51 mRNA and protein levels in primary HGPS fibroblasts by a dominant-negative mechanism rather than gain-of-function, likely due to inhibition of FLp53 resulting in the increased expression of E2F1, an activator of RAD51.

It has been well established that p53-induced accelerated senescence contributes to the aging-associated symptoms of HGPS patients and mouse models[24, 26]. Together with our results, these data indicate that progeroid phenotypes can be at least partially rescued by p53 signaling inhibition *in vitro* and *in vivo*. Our report is the first study that shows that an endogenous mechanism, i.e. Δ133p53 expression, can modulate FLp53 function and the p53-signaling pathway to inhibit the early onset of senescence in HGPS fibroblasts. We propose that by physically interacting with and dominant-negatively inhibiting FLp53, Δ133p53 represses the transcriptional activation of p53-target genes involved in senescence, promoting cellular proliferation of HGPS fibroblasts by inhibiting cell cycle checkpoints regulated by p53-target genes.

The role of Δ133p53 in DNA repair of spontaneous DNA damage caused by intrinsic cellular stresses, for instance, the cytotoxic effects of progerin in HGPS fibroblasts, was previously unknown. In this study, we show that Δ133p53 expression decreased the amount of DSBs accumulated in HGPS fibroblasts, indicating that the expression of this isoform may promote DNA repair in this premature aging syndrome. It is still unclear how progerin accumulation leads to DNA repair defects in HGPS fibroblasts. A recent study showed that defects in nuclear shape and lamin A production due to progerin accumulation result in entrapment the anti-oxidant transcription factor NRF2[19] and in defective assembly of repair foci, as evidenced by the previously reported progerin-induced defects in homologous recombination in HGPS[51] likely due to impaired recruitment of RAD51 to γH2AX foci in HGPS fibroblasts. In this scenario, our data show that Δ133p53 expression acts downstream of progerin and facilitates repair of progerin-induced DSBs by enhancing RAD51 cellular levels through inhibition of FLp53 and increase of the RAD51 activator E2F1.

The most common cause of death of HGPS children is cardiovascular disease[9, 56], possibly as a result of degeneration of vascular smooth muscle cells (VSMC)[57–59]. A previous study showed that differentiation of HGPS-derived induced pluripotent (iPSC) cells into VSMCs leads to increased DNA damage and accelerated senescence associated with vascular aging[14, 26, 59], possibly due to reprogramming of repressors induced by NF-kB hyperactivation[60]. Future investigations will address whether Δ133p53 is expressed during differentiation to VSMCs and whether restoration of its expression could be used to rescue

senescence of VSMCs and vascular aging. In this context, manipulation of endogenous Δ133p53 expression *in vivo* for instance, by using small molecules or drugs that modulate its regulatory mechanism, namely, chaperone-assisted selective autophagy, may be a therapeutic strategy of interest in HGPS.

MATERIALS AND METHODS

Cells, Cell Culture and Cell Treatment

Primary fibroblasts derived from a healthy patient or from three HGPS patients carrying the classic *LMNA* mutation (LMNA Exon 11, heterozygous c.1824C>T) were purchased from Coriell Cell Repositories and from Progeria Research Foundation (see Supplementary Table S1 for more details). Cells were cultured in DMEM medium supplemented with 10% fetal bovine serum, 2mM glutamine, and 50 IU/ml penicillin/streptomycin (Thermofisher, MA). The number of population doubling levels (PDLs) were calculated as log10(number of cells counted after expansion) – log10(number of cells seeded)/log2. Autophagy was inhibited by treating cells with 100nM of autophagy inhibitor bafilomycin A1 (Sigma-Aldrich, MO) for 4 hours. DMSO was used as a control.

Lentiviral transductions

pLenti6 (Open Biosystems, CO) were used to express Δ133p53. pQCXIN-FLAG-Δ133p53 and pQCXIN-FLAG-p53β were previously generated and reported[28]. Cells were transduced with 0.3-3 multiplicity of infection (MOI) and incubated with lentiviral supernatant for 24 hours, followed by media change. Transduced cells were selectrf with blasticidin (pLenti6 construct) or puromycin (pQCXIN construct) 48 hours after transduction and continued until approximately 80% of untransduced cells died.

SA-β-gal assay

To examine senescence, cells plated into wells of 6-well plates were fixed and stained using a Senescence β-Galactosidase Staining Kit (Cell Signaling, MA) following the manufacturer's instructions.

siRNA oligonucleotides and knockdown

siRNA transfections were performed using lipofectamine RNAiMax (Thermofisher, MA) as per manufacturer's instructions. siRNA oligonucleotides used for this study are listed in Supplementary Table S3.

Protein Lysate Preparation and Immunoblot Analysis

Cells were lysed in RIPA buffer containing phosphatase inhibitor. Protein lysates were separated by electrophoresis using 10% Tris-Glycine or 4-12% Bis-Tris gels (ThermoFisher, MA). Primary and secondary antibodies used are listed in Supplementary Table S4. Signals were with ECL detection (Amersham Biosciences, UK) or SuperSignal West Dura Extended Duration system (Thermofisher, MA) per the manufacturer's instructions. Quantification analysis was performed using ImageJ 1.42q software (http://rsb.info.nih.gov/ij/). β-actin was used as normalization control.

RNA isolation and Real-time qRT-PCR of mRNA expression

RNA samples were prepared using miRNeasy micro kit (QIAGEN, Catalog # 217084), and reverse transcriptase reaction was performed using High Capacity cDNA Reverse Transcription Kit (ThermoFisher, Catalog # 4368813). Taqman Universal PCR Master Mix (ThermoFisher Catalo # 4304437) or SyberGreen Master Mix (Thermofisher, Catalog # 4309155) were used with the Taqman assays or primer pairs for detection the specified genes listed in Supplementary Table S5 and S6, respectively. Normalized expression was calculated as relative fold change using the ΔΔCt method according to manufacturer's instructions (Applied Biosystems, protocol no. 4310255B, user bulletin no. 4303859B).

MicroRNA isolation and Quantitative Real Time PCR of microRNA expression

RNA samples prepared using miRNeasy micro kit (QIAGEN, Catalog # 217084) were used for reverse transcription reactions performed using TaqMan microRNA reverse transcription kit (Thermo Fisher, Catalog # 4366596) and a mir-34a-specific primer (RT/TM 425, Thermo Fisher, MA), according to the supplier's protocol. Three technical and biological replicates were measured. RNU66 (RT/TM 1002, Thermofisher, MA) was used as a control for normalization, and normalized expression of miR-34a was calculated as relative fold change by using the ΔΔCt method according to the supplier's protocol (protocol no. 4310255B and User Bulletin no. 4303859B at http://www.appliedbiosystems.com/index.cfm).

Immunocytochemistry

Approximately 2×10^4 cells plated onto coverslips in 24-well plates were stained with one or more antibodies using a standard protocol. Briefly, cells were fixed with 4% paraformaldehyde (PFA) in PBS for approximately 15 min on ice, followed by incubation with 0.25% Triton-X-100/PBS for cell permeabilization at room temperature (RT) for 10 min. Cells blocked for 1 hour with 1% bovine serum albumin (BSA) in PBS at RT were incubated overnight with primary antibodies in 1% BSA solution. For immunostaining of RAD51, cells were fixed in ice-cold methanol for 10 min at −20°C and permeabilized in 0.5% Triton-X-100/PBS on ice for 5 min. Antibodies used for immunostaining are listed in Supplementary Table S4. Alexa Fluor–conjugated secondary antibodies (1:400; Thermofisher, MA) were used for secondary staining for 1 hour at RT. Stained cells were mounted onto glass slides using Mounting Medium containing 4′,6-diamidino-2-phenylindole (catalog number H-1200, VECTASHIELD) for nuclear staining. Digital images were acquired using the confocal microscopes Zeiss 710 or Zeiss 780, and images were analyzed using ZEN (Zeiss) and Photoshop (Adobe). Quantification of γH2AX foci was performed using the automated software ImagePremier Pro. Co-localization of γH2AX-positive DSBs with RAD51 was quantified and DSBs were scored as RAD51-positive (RAD51+ve) or RAD51-negative (RAD51-ve). At least 100 cells were counted per experiment.

Chromatin immunoprecipitation (ChIP)

BJ cells cultured in 10 cm plates were used for immunoprecipitation. Cells were fixed with 1% formaldehyde for 15 min at room temperature with gentle agitation, followed by addition of glycine to a final concentration of 0.125 M, and incubated for 10 min at room

temperature. Harvested cells were resuspended in 1 ml of SDS lysis buffer (1% SDS, 50 mM Tris-HCl (pH 8.0), 10 mM EDTA, and complete EDTA-free protease inhibitors (Sigma 11697498001). Following sonication, samples were centrifuged at 14,000 rpm at 8°C for 10 min. Supernatants, diluted ten-fold in ChIP dilution buffer (1% TritonX-100, 20 mM Tris-HCl (pH 8.0), 150 mM NaCl, 2 mM EDTA, complete EDTA-free protease inhibitors), were incubated at 4°C overnight with anti-mouse IgG-Dynabeads following pre-incubation with 5 μg of Do-1 antibodies in PBS / 0.5% BSA. Beads were transferred to 1.5 ml DNA Lo-bind tubes (Eppendolf 030108051), and were washed with ChIP wash buffer (0.7% DOC, 1% NP-40, 50 mM HEPES- KOH (pH 7.0), 0.5 M LiCl, 1 mM EDTA) and with TE buffer (pH 8.0). Elution of immunoprecipites was followed by incubation overnight at 65 °C in elution buffer (1% SDS, 50 mM Tris-HCl (pH 8.0), 10 mM EDTA) for reverse-crosslinking. Genomic DNA extracted with a PCR purification kit (Qiagen) was used for qPCR analysis with PowerUP SYBR Green Master Mix (Thermo Fisher, A25742). Triplicates of each sample were run and averaged.

Statistics

Statistical analyses of three independent experiments were performed using 2-tailed Student's t test. P values lower than 0.05 were valued as significant.

Supplementary Material

Refer to Web version on PubMed Central for supplementary material.

Acknowledgments

We thank Tom Misteli for kindly providing reagents and materials. We are grateful to Madaiah Puttaraju, who provided technical assistance with quantitative real time PCR of progerin and wild-type lamin A. We would like to thank Dr. Ana Robles for critical reading of the manuscript. Confocal microscopy was supported by the National Cancer Institute. This research was supported by the Intramural Research Program of the NIH, NCI.

FUNDING: This work was funded by the National Cancer Institute, National Institutes of Health. B.V. was supported with project from Czech Science Foundation P206/12/G151 and project MEYS - NPS I - LO1413.

References

1. Allsopp RC, Vaziri H, Patterson C, Goldstein S, Younglai EV, Futcher AB, et al. Telomere length predicts replicative capacity of human fibroblasts. Proc Natl Acad Sci U S A. 1992; 89:10114–10118. [PubMed: 1438199]
2. Sedelnikova OA, Horikawa I, Zimonjic DB, Popescu NC, Bonner WM, Barrett JC. Senescing human cells and ageing mice accumulate DNA lesions with unrepairable double-strand breaks. Nat Cell Biol. 2004; 6:168–170. [PubMed: 14755273]
3. Munoz-Espin D, Serrano M. Cellular senescence: from physiology to pathology. Nat Rev Mol Cell Biol. 2014; 15:482–496. [PubMed: 24954210]
4. Lopez-Otin C, Blasco MA, Partridge L, Serrano M, Kroemer G. The hallmarks of aging. Cell. 2013; 153:1194–1217. [PubMed: 23746838]
5. Campisi J, Robert L. Cell senescence: role in aging and age-related diseases. Interdiscip Top Gerontol. 2014; 39:45–61. [PubMed: 24862014]
6. Kudlow BA, Kennedy BK, Monnat RJ Jr. Werner and Hutchinson-Gilford progeria syndromes: mechanistic basis of human progeroid diseases. Nat Rev Mol Cell Biol. 2007; 8:394–404. [PubMed: 17450177]

7. Opresko PL, von Kobbe C, Laine JP, Harrigan J, Hickson ID, Bohr VA. Telomere-binding protein TRF2 binds to and stimulates the Werner and Bloom syndrome helicases. J Biol Chem. 2002; 277:41110–41119. [PubMed: 12181313]
8. Burtner CR, Kennedy BK. Progeria syndromes and ageing: what is the connection? Nat Rev Mol Cell Biol. 2010; 11:567–578. [PubMed: 20651707]
9. Hennekam RC. Hutchinson-Gilford progeria syndrome: review of the phenotype. Am J Med Genet A. 2006; 140:2603–2624. [PubMed: 16838330]
10. Pereira S, Bourgeois P, Navarro C, Esteves-Vieira V, Cau P, De Sandre-Giovannoli A, et al. HGPS and related premature aging disorders: from genomic identification to the first therapeutic approaches. Mech Ageing Dev. 2008; 129:449–459. [PubMed: 18513784]
11. De Sandre-Giovannoli A, Bernard R, Cau P, Navarro C, Amiel J, Boccaccio I, et al. Lamin a truncation in Hutchinson-Gilford progeria. Science. 2003; 300:2055. [PubMed: 12702809]
12. Eriksson M, Brown WT, Gordon LB, Glynn MW, Singer J, Scott L, et al. Recurrent de novo point mutations in lamin A cause Hutchinson-Gilford progeria syndrome. Nature. 2003; 423:293–298. [PubMed: 12714972]
13. Goldman RD, Shumaker DK, Erdos MR, Eriksson M, Goldman AE, Gordon LB, et al. Accumulation of mutant lamin A causes progressive changes in nuclear architecture in Hutchinson-Gilford progeria syndrome. Proc Natl Acad Sci U S A. 2004; 101:8963–8968. [PubMed: 15184648]
14. Scaffidi P, Misteli T. Lamin A-dependent misregulation of adult stem cells associated with accelerated ageing. Nat Cell Biol. 2008; 10:452–459. [PubMed: 18311132]
15. Malhas AN, Lee CF, Vaux DJ. Lamin B1 controls oxidative stress responses via Oct-1. J Cell Biol. 2009; 184:45–55. [PubMed: 19139261]
16. Shumaker DK, Dechat T, Kohlmaier A, Adam SA, Bozovsky MR, Erdos MR, et al. Mutant nuclear lamin A leads to progressive alterations of epigenetic control in premature aging. Proc Natl Acad Sci U S A. 2006; 103:8703–8708. [PubMed: 16738054]
17. Vidak S, Kubben N, Dechat T, Foisner R. Proliferation of progeria cells is enhanced by lamina-associated polypeptide 2alpha (LAP2alpha) through expression of extracellular matrix proteins. Genes Dev. 2015; 29:2022–2036. [PubMed: 26443848]
18. McCord RP, Nazario-Toole A, Zhang H, Chines PS, Zhan Y, Erdos MR, et al. Correlated alterations in genome organization, histone methylation, and DNA-lamin A/C interactions in Hutchinson-Gilford progeria syndrome. Genome Res. 2013; 23:260–269. [PubMed: 23152449]
19. Kubben N, Zhang W, Wang L, Voss TC, Yang J, Qu J, et al. Repression of the Antioxidant NRF2 Pathway in Premature Aging. Cell. 2016; 165:1361–1374. [PubMed: 27259148]
20. Gonzalo S, Kreienkamp R. DNA repair defects and genome instability in Hutchinson-Gilford Progeria Syndrome. Curr Opin Cell Biol. 2015; 34:75–83. [PubMed: 26079711]
21. Musich PR, Zou Y. Genomic instability and DNA damage responses in progeria arising from defective maturation of prelamin A. Aging (Albany NY). 2009; 1:28–37. [PubMed: 19851476]
22. Musich PR, Zou Y. DNA-damage accumulation and replicative arrest in Hutchinson-Gilford progeria syndrome. Biochem Soc Trans. 2011; 39:1764–1769. [PubMed: 22103522]
23. Liu B, Wang J, Chan KM, Tjia WM, Deng W, Guan X, et al. Genomic instability in laminopathy-based premature aging. Nat Med. 2005; 11:780–785. [PubMed: 15980864]
24. Varela I, Cadinanos J, Pendas AM, Gutierrez-Fernandez A, Folgueras AR, Sanchez LM, et al. Accelerated ageing in mice deficient in Zmpste24 protease is linked to p53 signalling activation. Nature. 2005; 437:564–568. [PubMed: 16079796]
25. Liu Y, Rusinol A, Sinensky M, Wang Y, Zou Y. DNA damage responses in progeroid syndromes arise from defective maturation of prelamin A. J Cell Sci. 2006; 119:4644–4649. [PubMed: 17062639]
26. Osorio FG, Navarro CL, Cadinanos J, Lopez-Mejia IC, Quiros PM, Bartoli C, et al. Splicing-directed therapy in a new mouse model of human accelerated aging. Sci Transl Med. 2011; 3:106ra107.
27. Khoury MP, Bourdon JC. The isoforms of the p53 protein. Cold Spring Harb Perspect Biol. 2010; 2:a000927. [PubMed: 20300206]

28. Fujita K, Mondal AM, Horikawa I, Nguyen GH, Kumamoto K, Sohn JJ, et al. p53 isoforms Delta133p53 and p53beta are endogenous regulators of replicative cellular senescence. Nat Cell Biol. 2009; 11:1135–1142. [PubMed: 19701195]
29. Mondal AM, Horikawa I, Pine SR, Fujita K, Morgan KM, Vera E, et al. p53 isoforms regulate aging- and tumor-associated replicative senescence in T lymphocytes. J Clin Invest. 2013; 123:5247–5257. [PubMed: 24231352]
30. Turnquist C, Horikawa I, Foran E, Major EO, Vojtesek B, Lane DP, et al. p53 isoforms regulate astrocyte-mediated neuroprotection and neurodegeneration. Cell Death Differ. 2016
31. Horikawa I, Park KY, Isogaya K, Hiyoshi Y, Li H, Anami K, et al. Delta133p53 represses p53-inducible senescence genes and enhances the generation of human induced pluripotent stem cells. Cell Death Differ. 2017; 24:1017–1028. [PubMed: 28362428]
32. Bourdon JC, Fernandes K, Murray-Zmijewski F, Liu G, Diot A, Xirodimas DP, et al. p53 isoforms can regulate p53 transcriptional activity. Genes Dev. 2005; 19:2122–2137. [PubMed: 16131611]
33. Maki CG, Huibregtse JM, Howley PM. In vivo ubiquitination and proteasome-mediated degradation of p53(1). Cancer Res. 1996; 56:2649–2654. [PubMed: 8653711]
34. Haupt Y, Maya R, Kazaz A, Oren M. Mdm2 promotes the rapid degradation of p53. Nature. 1997; 387:296–299. [PubMed: 9153395]
35. Horikawa I, Fujita K, Jenkins LM, Hiyoshi Y, Mondal AM, Vojtesek B, et al. Autophagic degradation of the inhibitory p53 isoform Delta133p53alpha as a regulatory mechanism for p53-mediated senescence. Nat Commun. 2014; 5:4706. [PubMed: 25144556]
36. Tang Y, Horikawa I, Ajiro M, Robles AI, Fujita K, Mondal AM, et al. Downregulation of splicing factor SRSF3 induces p53beta, an alternatively spliced isoform of p53 that promotes cellular senescence. Oncogene. 2013; 32:2792–2798. [PubMed: 22777358]
37. Gong L, Gong H, Pan X, Chang C, Ou Z, Ye S, et al. p53 isoform Delta113p53/Delta133p53 promotes DNA double-strand break repair to protect cell from death and senescence in response to DNA damage. Cell Res. 2015; 25:351–369. [PubMed: 25698579]
38. Yanez RJ, Porter AC. Gene targeting is enhanced in human cells overexpressing hRAD51. Gene Ther. 1999; 6:1282–1290. [PubMed: 10455437]
39. Wu M, Wang X, McGregor N, Pienta KJ, Zhang J. Dynamic regulation of Rad51 by E2F1 and p53 in prostate cancer cells upon drug-induced DNA damage under hypoxia. Mol Pharmacol. 2014; 85:866–876. [PubMed: 24627085]
40. Arias-Lopez C, Lazaro-Trueba I, Kerr P, Lord CJ, Dexter T, Iravani M, et al. p53 modulates homologous recombination by transcriptional regulation of the RAD51 gene. EMBO Rep. 2006; 7:219–224. [PubMed: 16322760]
41. Mizushima N, Levine B, Cuervo AM, Klionsky DJ. Autophagy fights disease through cellular self-digestion. Nature. 2008; 451:1069–1075. [PubMed: 18305538]
42. Aoubala M, Murray-Zmijewski F, Khoury MP, Fernandes K, Perrier S, Bernard H, et al. p53 directly transactivates Delta133p53alpha, regulating cell fate outcome in response to DNA damage. Cell Death Differ. 2011; 18:248–258. [PubMed: 20689555]
43. Wei J, Noto J, Zaika E, Romero-Gallo J, Correa P, El-Rifai W, et al. Pathogenic bacterium Helicobacter pylori alters the expression profile of p53 protein isoforms and p53 response to cellular stresses. Proc Natl Acad Sci U S A. 2012; 109:E2543–2550. [PubMed: 22927405]
44. Shieh SY, Ikeda M, Taya Y, Prives C. DNA damage-induced phosphorylation of p53 alleviates inhibition by MDM2. Cell. 1997; 91:325–334. [PubMed: 9363941]
45. Brown JP, Wei W, Sedivy JM. Bypass of senescence after disruption of p21CIP1/WAF1 gene in normal diploid human fibroblasts. Science. 1997; 277:831–834. [PubMed: 9242615]
46. Herbig U, Jobling WA, Chen BP, Chen DJ, Sedivy JM. Telomere shortening triggers senescence of human cells through a pathway involving ATM, p53, and p21(CIP1), but not p16(INK4a). Mol Cell. 2004; 14:501–513. [PubMed: 15149599]
47. Sedelnikova OA, Horikawa I, Redon C, Nakamura A, Zimonjic DB, Popescu NC, et al. Delayed kinetics of DNA double-strand break processing in normal and pathological aging. Aging Cell. 2008; 7:89–100. [PubMed: 18005250]

48. d'Adda di Fagagna F, Reaper PM, Clay-Farrace L, Fiegler H, Carr P, Von Zglinicki T, et al. A DNA damage checkpoint response in telomere-initiated senescence. Nature. 2003; 426:194–198. [PubMed: 14608368]

49. Zhang H, Xiong ZM, Cao K. Mechanisms controlling the smooth muscle cell death in progeria via down-regulation of poly(ADP-ribose) polymerase 1. Proc Natl Acad Sci U S A. 2014; 111:E2261–2270. [PubMed: 24843141]

50. Sung P. Catalysis of ATP-dependent homologous DNA pairing and strand exchange by yeast RAD51 protein. Science. 1994; 265:1241–1243. [PubMed: 8066464]

51. Liu Y, Wang Y, Rusinol AE, Sinensky MS, Liu J, Shell SM, et al. Involvement of xeroderma pigmentosum group A (XPA) in progeria arising from defective maturation of prelamin A. FASEB J. 2008; 22:603–611. [PubMed: 17848622]

52. Linke SP, Sengupta S, Khabie N, Jeffries BA, Buchhop S, Miska S, et al. p53 interacts with hRAD51 and hRAD54, and directly modulates homologous recombination. Cancer Res. 2003; 63:2596–2605. [PubMed: 12750285]

53. Buchhop S, Gibson MK, Wang XW, Wagner P, Sturzbecher HW, Harris CC. Interaction of p53 with the human Rad51 protein. Nucleic Acids Res. 1997; 25:3868–3874. [PubMed: 9380510]

54. Brosh R, Shalgi R, Liran A, Landan G, Korotayev K, Nguyen GH, et al. p53-Repressed miRNAs are involved with E2F in a feed-forward loop promoting proliferation. Mol Syst Biol. 2008; 4:229. [PubMed: 19034270]

55. Kachhap SK, Rosmus N, Collis SJ, Kortenhorst MS, Wissing MD, Hedayati M, et al. Downregulation of homologous recombination DNA repair genes by HDAC inhibition in prostate cancer is mediated through the E2F1 transcription factor. PLoS One. 2010; 5:e11208. [PubMed: 20585447]

56. Merideth MA, Gordon LB, Clauss S, Sachdev V, Smith AC, Perry MB, et al. Phenotype and course of Hutchinson-Gilford progeria syndrome. N Engl J Med. 2008; 358:592–604. [PubMed: 18256394]

57. Varga R, Eriksson M, Erdos MR, Olive M, Harten I, Kolodgie F, et al. Progressive vascular smooth muscle cell defects in a mouse model of Hutchinson-Gilford progeria syndrome. Proc Natl Acad Sci U S A. 2006; 103:3250–3255. [PubMed: 16492728]

58. Olive M, Harten I, Mitchell R, Beers JK, Djabali K, Cao K, et al. Cardiovascular pathology in Hutchinson-Gilford progeria: correlation with the vascular pathology of aging. Arterioscler Thromb Vasc Biol. 2010; 30:2301–2309. [PubMed: 20798379]

59. Ragnauth CD, Warren DT, Liu Y, McNair R, Tajsic T, Figg N, et al. Prelamin A acts to accelerate smooth muscle cell senescence and is a novel biomarker of human vascular aging. Circulation. 2010; 121:2200–2210. [PubMed: 20458013]

60. Soria-Valles C, Osorio FG, Gutierrez-Fernandez A, De Los Angeles A, Bueno C, Menendez P, et al. NF-kappaB activation impairs somatic cell reprogramming in ageing. Nat Cell Biol. 2015; 17:1004–1013. [PubMed: 26214134]

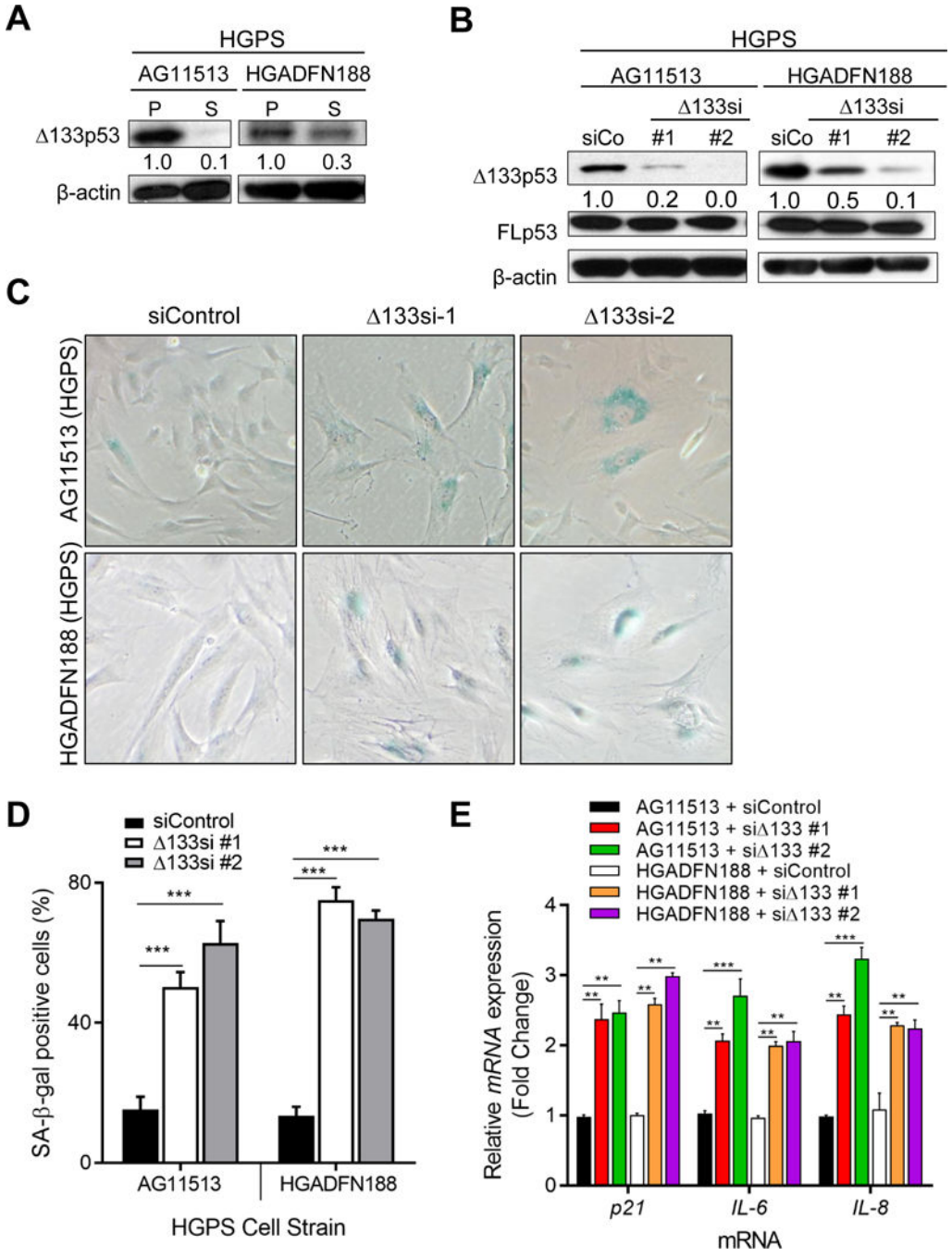

Figure 1. Δ133p53 is an endogenous regulator of cellular senescence in HGPS fibroblasts

AG11513 and HGADFN188 fibroblasts derived from two HGPS patients were used. **(A)** Proliferative (P) and replicative senescent (S) HGPS cells were analyzed by immunoblot using MAP4 antibody for Δ133p53 expression. β-actin was used as loading control. Image J was used for quantification. AG11513 at passage 8 (P) and 15 (S) and HGADFN188 at passage 10 (P) and 19 (S) were examined. **(B-E)** Proliferative HGPS fibroblasts (AG11513, passage 9; HGADFN188, passage 10) were transfected with one of two Δ133p53 siRNAs (Δ133si-1 or Δ133si -2) or a control siRNA every 3-5 days. Cells were analyzed at day 10.

(B) Immunoblot to compare the expression of the indicated proteins in HGPS fibroblasts. Δ133p53 and full-length p53 (FLp53) were detected using MAP4 and DO-1 antibodies, respectively. β-actin was used as a loading control. Image J was used for quantification. **(C)** Representative images of senescence-associated β-galactosidase (SA-β-gal) staining of HGPS cells transfected with Δ133p53-specific siRNA. **(D)** Quantification of SA-β-gal positive cells transfected with the indicated siRNAs. At least 100 cells were counted per experiment. The data are mean ± s.d. from three independent experiments. *** $P < 0.001$. **(E)** Quantification of mRNA expression of the p53-target gene *p21* and the senescence-associated secretory phenotype (SASP) pro-inflammatory cytokines interleukin 6 (IL6) and interleukin 8 (IL-8) by quantitative real time PCR (qRT-PCR) in cells transfected with the indicated siRNAs. B2M was used for normalization. The data are mean ± s.d. from three independent experiments. ** $P < 0.01$; *** $P < 0.001$.

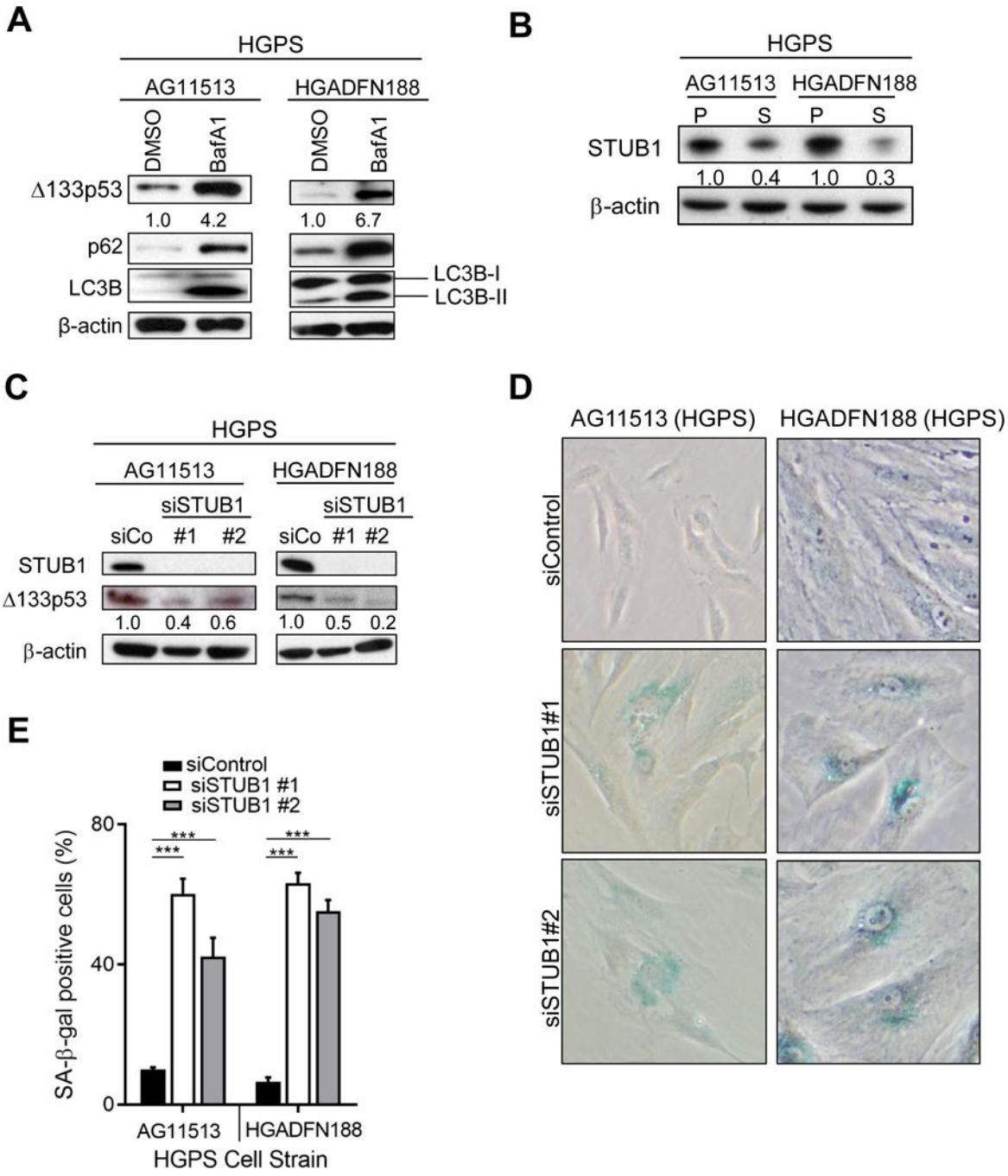

Figure 2. Δ133p53 is regulated by selective autophagy in HGPS fibroblasts

(**A**) Immunoblot of bafilomycin A1 (bafA1)-treated near-senescent HGPS fibroblasts (AG11513 or HGADFN188). Δ133p53 was detected using MAP4 antibody. Autophagy inhibition was confirmed by accumulation of the autophagy-related proteins p62 and LC3B-II in bafilomycin A1 (bafA1)-containing media. β-actin was used as a loading control. Image J was used for quantification of Δ133p53. **(B)** Immunoblot of STUB1, a regulator of selective autophagy of Δ133p53 (Horikawa et al, 2014) in proliferative (P) and senescent (S) HGPS fibroblasts. AG11513 fibroblasts were examined at passage 9 (P) and passage 15 (S)

while HGADFN188 cells were analyzed at passage 10 (P) and 19 (S). **(C,D)** siRNA-mediated knockdown of STUB1. **(C)** STUB1 and Δ133p53 were detected by immunoblot in siRNA-transfected cells. β-actin was used as a loading control. Quantification, performed with Image J, is summarized below. **(D)** Summary of quantification of SA-β-gal staining of siRNA-transfected cells. The data are mean ± s.d. from three independent experiments. *** $P < 0.001$.

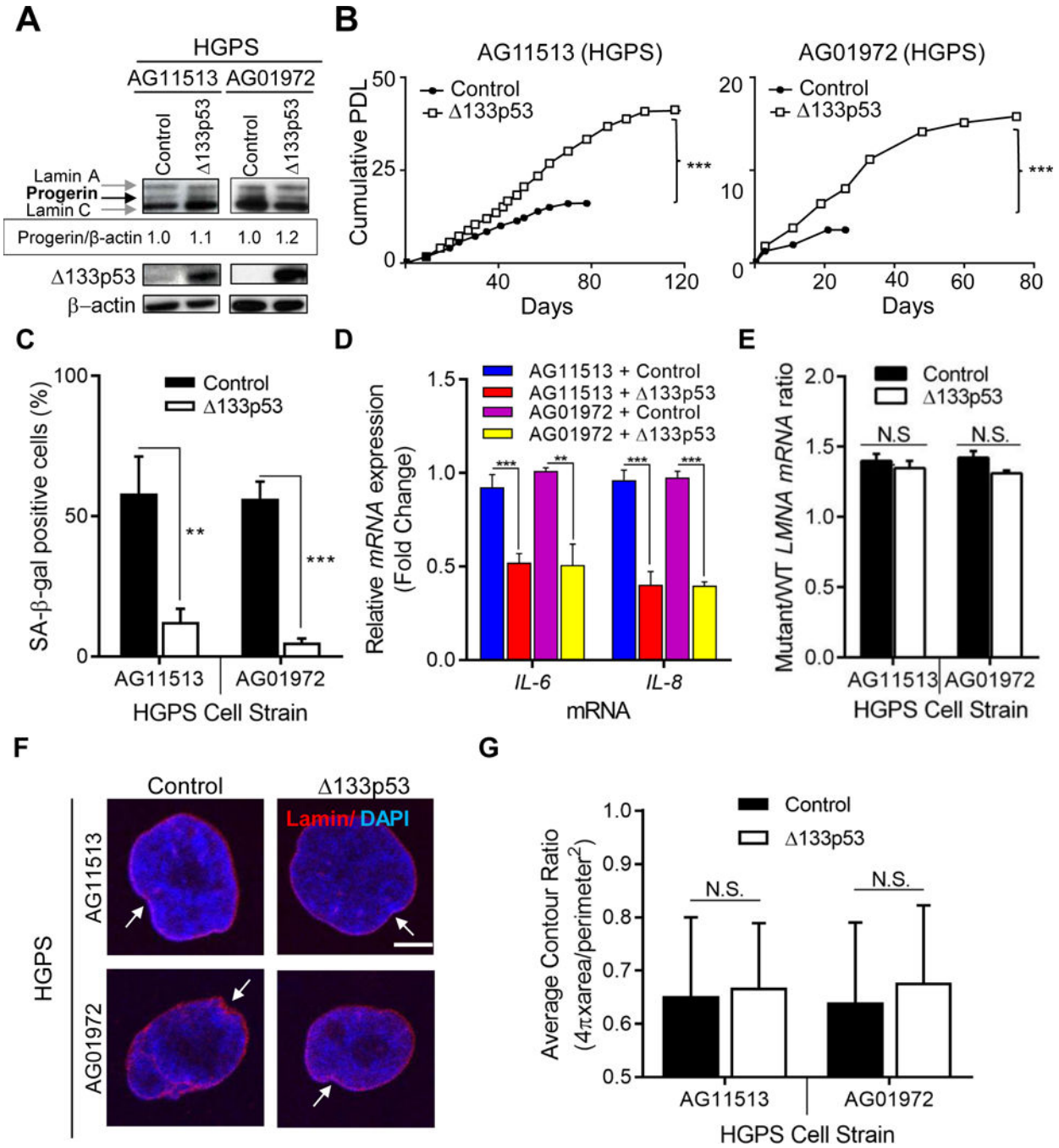

Figure 3. Overexpression of Δ133p53 extends the replicative lifespan and delays the onset of senescence by a mechanism downstream of progerin or nuclear abnormalities in fibroblasts derived from HGPS patients

HGPS fibroblasts approaching replicative senescence AG11513 (passage 10) and AG01972 (passage 16), were transduced with either Δ133p53- or control- lentiviral vector and selected using blasticidin-containing media. (**A**) Immunoblot of Δ133p53 isoform and progerin, detected with N-18, a polyclonal antibody that recognizes an epitope in the N-terminus of lamin A, progerin and lamin C, respectively. Quantification performed with Image J and summarized below. β-actin was used as a loading control. (**B**) Cumulative population

doublings (PDL) were analyzed until cells reached proliferation arrest and became senescent. Three wells were counted per experiment. The data are mean ± s.d. from three independent experiments. *** $P < 0.001$. (**C-G**) Transduced HGPS fibroblasts were analyzed approximately 7-10 days after selection with blasticidin. Control- and Δ133p53-transduced wells were stained (**C**), harvested (**D,E**) or fixed (**F**) the same day. AG11513 (HGPS) fibroblasts expressing control or Δ133p53 were analyzed at passage 12 and 14, respectively. AG01972 (HGPS) fibroblasts expressing control or Δ133p53 vector were analyzed at passage 18 and 20, respectively. (**C**) Quantification of SA-β-gal-positive cells is shown. (**D**) Quantitative real time PCR for *IL-6* and *IL-8*. B2M was used for normalization. (**E**) Quantitative real time PCR progerin (mutant) or wild-type (WT) *LMNA*. Ratio of mutant and WT *LMNA* expression shown. (**F,G**) Immunostaining of the nuclear lamina using N-18 antibody of the indicated transduced cells. 4′,6-diamidino-2-phenylindole (DAPI) was used to stain the nucleus. Scale bar= 10μm. (**G**) Average contour ratio, used as an index of abnormal nuclear morphology, was calculated for the indicated cells. ImagePro Premier was used to determine the cellular area and perimeter. Data are mean ± s.d. from three independent experiments. ** $P < 0.01$; *** $P < 0.001$. N.S. Non-significant.

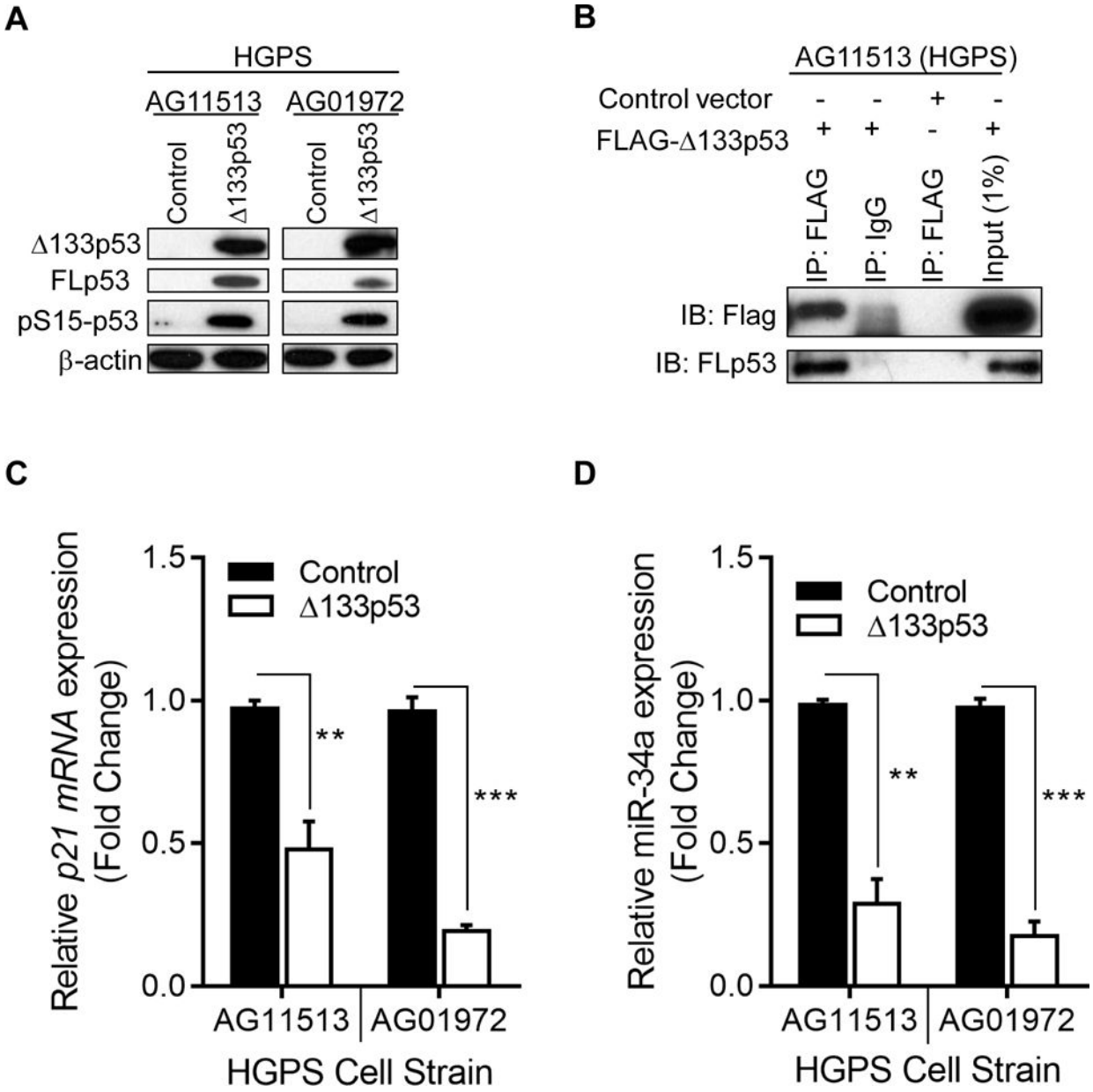

Figure 4. Overexpression of Δ133p53 results in Inhibition of p53 signaling due to its interaction with full-length p53 (FLp53) in HGPS fibroblasts

(**A,C,D**) AG11513 and AG01972 HGPS fibroblasts were transduced with Δ133p53- or control- lentiviral vectors as in Figure 3. (**A**) Overexpression of Δ133p53 was confirmed using MAP4 antibody. Full-length p53 (FLp53) was detected using DO-1 antibody. FLp53 phosphorylated at Ser 15 (pS15-p53) was also analyzed. (**B**) Immunoprecipitation of FLAG-tagged Δ133p53 expressed in AG11513 (HGPS) fibroblasts using anti-FLAG antibody bound to agarose beads. The resulting immunoprecipitants were analyzed by western blot using the indicated antibodies. (**C,D**) Quantitative real time PCR of (**C**) *p21/CDKN1A* and (**D**) miR-34a, endogenous regulators of replicative senescence. The data are mean ± s.d. from three independent experiments. ** $P < 0.01$; *** $P < 0.001$.

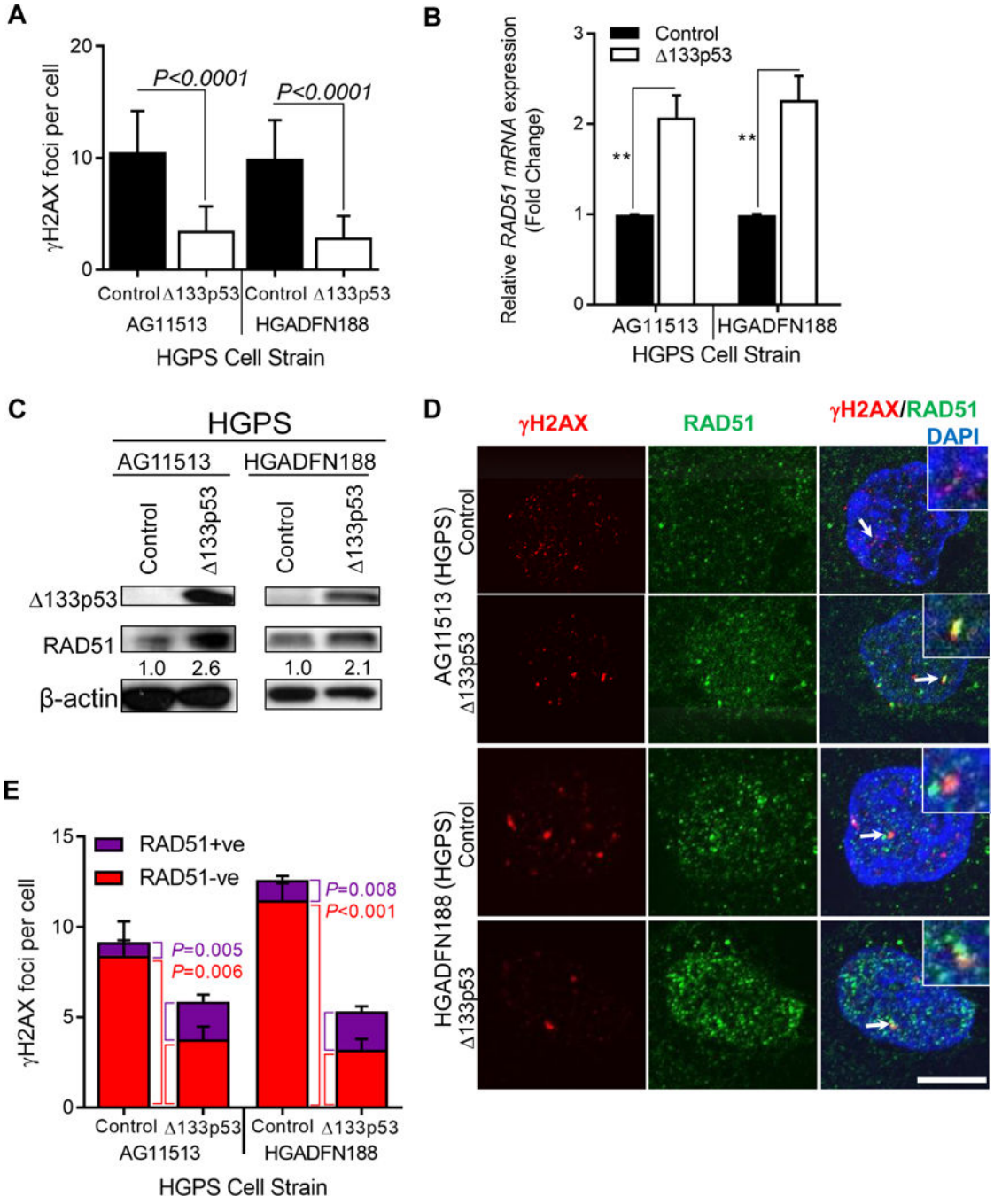

Figure 5. Δ133p53 expression results in decreased DNA double-strand break (DSB) foci in HGPS fibroblasts

HGPS fibroblasts approaching replicative senescence AG11513 at passage 10 and HGADFN188 at passage 12 were transduced with Δ133p53- or control- lentiviral vectors. Control- and Δ133p53-expressing AG11513 were analyzed at passage 12 and 14, respectively. Control- and Δ133p53-expressing HGADFN188 were analyzed at passage 14 and 16, respectively. **(A)** Quantitative real time PCR of *RAD51*, a DNA repair factor involved in homologous recombination (HR). **(B)** Immunoblot of Δ133p53 and RAD51.

Quantification performed with Image J is shown below. Data are mean ± s.d. from three independent experiments. ** $P < 0.01$. **(C)** Quantification of phosphorylated H2AX (γH2AX) foci to detect DNA damage foci in HGPS fibroblasts expressing vector control or Δ133p53 (representative images in Supplementary Figure 9). Quantification of γH2AX foci was performed using ImagePremier Pro to detect foci. At least 100 cells were counted per experiment **(D,E)** HGPS fibroblasts were co-immunostained with antibodies to γH2AX (red) and RAD51 (green). 4′,6-diamidino-2-phenylindole (DAPI, blue) was used to stain the nucleus. **(D)** Representative images are shown. Images were taken using Zeiss LSM 780 confocal microscope. The area indicated by the white arrow was magnified (right panel). Scale bar= 5μm. **(E)** Quantification summary of RAD51 recruitment to γH2AX foci. γH2AX foci per cell were quantified. RAD51-positive (RAD51+ve) and RAD51-negative (RAD51-ve) γH2AX foci were quantified. The area inside the columns represents RAD51+ve (purple) or RAD51-ve (red) γH2AX foci. Data are mean ± s.d. from three independent experiments. *P* values were calculated comparing the RAD51+ve γH2AX foci (purple) or RAD51-negative (red) γH2AX foci in control- vs Δ133p53-expressing HGPS fibroblasts.

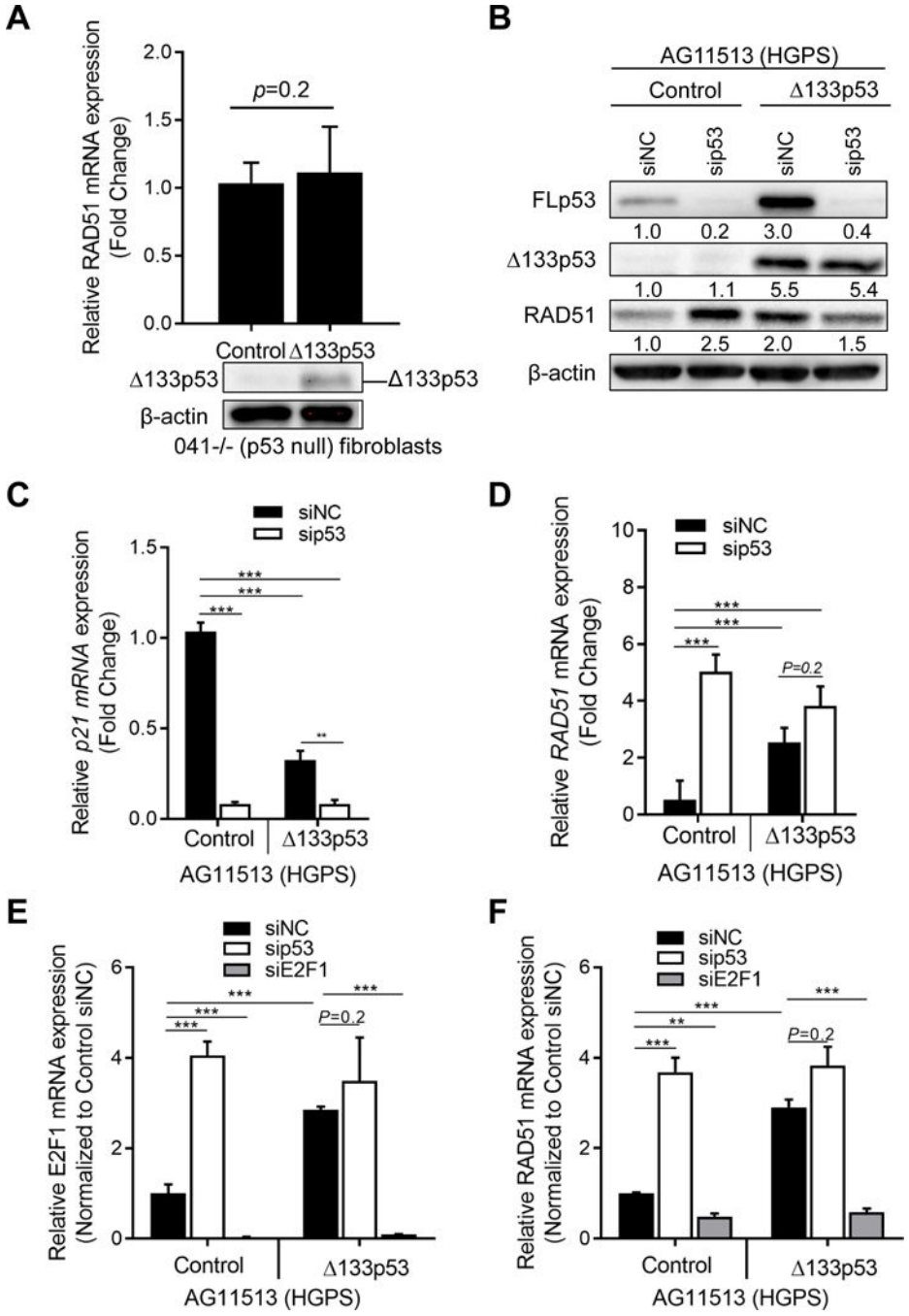

Figure 6. Δ133p53 dominant-negative inhibition of FLp53 results in increased RAD51 expression

(**A**) 041−/− fibroblasts (p53-null) were transduced with control- or Δ133p53- lentiviral supernatant. RAD51 mRNA expression was analyzed by quantitative RT-PCR. No significant change in RAD51 mRNA expression was detected in Δ133p53-expressing cells. Expression of Δ133p53 was confirmed by western blot. GAPDH was used for normalization. **(B-E)** AG11513 (HGPS) fibroblasts stably expressing a control or Δ133p53- lentiviral vector at passage 12-14 were transfected with siRNA targeting p53 (sip53), the transcription factor E2F1 (siE2F1) or a negative control (siNC). Cell pellets were collected 5

days after siRNA transfection. **(B)** Knockdown of FLp53, which does not change the expression Δ133p53, was confirmed by Western Blot. RAD51 protein expression was analyzed in the siRNA-transfected samples. Quantification was performed using Image J. β-actin was used as loading control. Relative expression of the indicated proteins in each siRNA-transfected sample was normalized to that of control-transduced HGPS fibroblasts transfected with negative control siRNA (siNC). **(C-F)** mRNA expression of the **(C)** senescence-associated gene *p21/CDKN1A*, **(D,F)** DNA repair factor *RAD51* and **(E)** transcription factor *E2F1* was analyzed by quantitative RT-PCR. GAPDH was used for normalization. Relative expression was normalized to control-transduced HGPS fibroblasts transfected with negative control siRNA (siNC). The data are mean ± s.d. from three independent experiments. ** $P < 0.01$; *** $P < 0.001$.

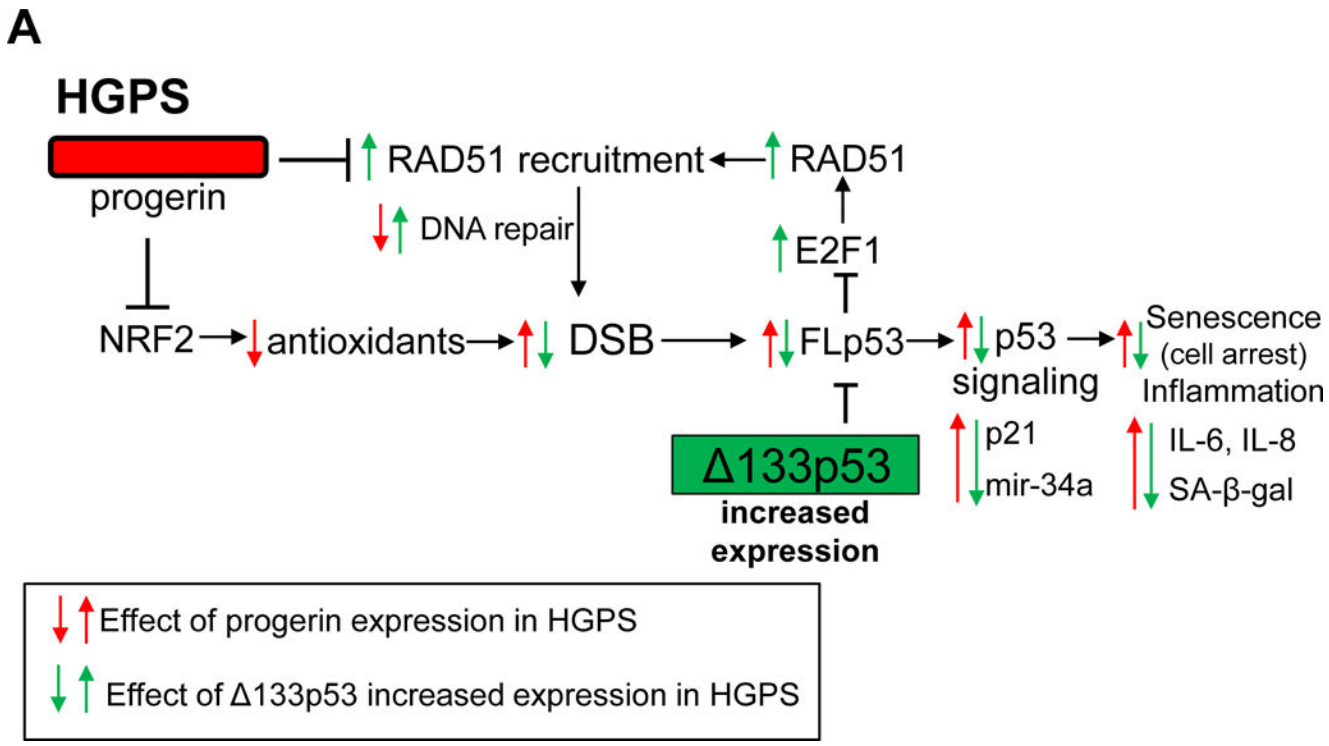

Figure 7. Model of Δ133p53 effects on DNA damage and senescence in HGPS fibroblasts

(**A**) Constitutive expression of progerin in HGPS leads to defects in the DNA repair machinery exacerbated by impaired activity of NRF2 pathway and increased oxidative stress among other cellular stresses, which result in accumulation of double strand breaks (DSB), p53 signaling activation, accelerated senescence and increased inflammation. Expression of Δ133p53, otherwise diminished in HGPS fibroblasts approaching proliferation arrest, dominant-negatively inhibits FLp53 leading to a delay of cellular senescence as evidenced by diminished staining of SA-β-galactosidase (SA-β-gal) and reduced expression of pro-inflammatory cytokines (IL-6 and IL-8) and the p53-target genes *p21/CDKN1A* and mir-34a. Furthermore, Δ133p53 overexpression indirectly increases the expression of the DNA repair factor RAD51 by dominant-negatively inhibiting FLp53 and increasing E2F1 expression levels, leading to a decrease in DNA damage foci. Effects of progerin expression in HGPS are depicted with red arrows, while effects of overexpression of Δ133p53 protein are indicated with green arrows.